

Extracellular Release of ILEI/FAM3C and Amyloid- β Is Associated with the Activation of Distinct Synapse Subpopulations

Masaki Nakano^a, Yachiyo Mitsuishi^a, Lei Liu^{a,1}, Naoki Watanabe^a, Emi Hibino^a, Saori Hata^{b,c}, Takashi Saito^{d,e}, Takaomi C. Saido^d, Shigeo Murayama^{f,2}, Kensaku Kasuga^g, Takeshi Ikeuchi^g, Toshiharu Suzuki^b and Masaki Nishimura^{a,*}

^a*Molecular Neuroscience Research Center, Shiga University of Medical Science, Shiga, Japan*

^b*Laboratory of Neuroscience, Graduate School of Pharmaceutical Sciences, Hokkaido University, Hokkaido, Japan*

^c*Biomedical Research Institute, National Institute of Advanced Industrial Science and Technology (AIST), Tsukuba, Japan*

^d*Laboratory for Proteolytic Neuroscience, RIKEN Brain Science Institute, Saitama, Japan*

^e*Department of Neurocognitive Science, Institute of Brain Science, Nagoya City University Graduate School of Medical Science, Nagoya, Japan*

^f*Department of Neurology and Neuropathology (the Brain Bank for Aging Research), Tokyo Metropolitan Geriatric Hospital and Institute of Gerontology, Tokyo, Japan*

^g*Department of Molecular Genetics, Brain Research Institute, Niigata University, Niigata, Japan*

Handling Associate Editor: Shun Shimohama

Accepted 16 December 2020

Pre-press 21 January 2021

Abstract.

Background: Brain amyloid- β (A β) peptide is released into the interstitial fluid (ISF) in a neuronal activity-dependent manner, and A β deposition in Alzheimer's disease (AD) is linked to baseline neuronal activity. Although the intrinsic mechanism for A β generation remains to be elucidated, interleukin-like epithelial-mesenchymal transition inducer (ILEI) is a candidate for an endogenous A β suppressor.

Objective: This study aimed to access the mechanism underlying ILEI secretion and its effect on A β production in the brain.

Methods: ILEI and A β levels in the cerebral cortex were monitored using a newly developed ILEI-specific ELISA and *in vivo* microdialysis in mutant human A β precursor protein-knockin mice. ILEI levels in autopsied brains and cerebrospinal fluid (CSF) were measured using ELISA.

Results: Extracellular release of ILEI and A β was dependent on neuronal activation and specifically on tetanus toxin-sensitive exocytosis of synaptic vesicles. However, simultaneous monitoring of extracellular ILEI and A β revealed that a spontaneous fluctuation of ILEI levels appeared to inversely mirror that of A β levels. Selective activation and inhibition of synaptic

¹Present address: Ann Romney Center for Neurologic Diseases, Brigham and Women's Hospital, Harvard Medical School, Boston, MA, USA.

²Present address: Brain Bank for Neurodevelopmental, Neurological and Psychiatric Disorders, United Graduate School of

Child, Development, Osaka University, Osaka, Japan.

*Correspondence to: Masaki Nishimura, Molecular Neuroscience Research Center, Shiga University of Medical Science, Shiga, 520 2192, Japan. Tel.: +81 77 548 2328; Fax: +81 77 548 2210; E-mail: mnishimu@belle.shiga-med.ac.jp.

receptors differentially altered these levels. The evoked activation of AMPA-type receptors resulted in opposing changes to ILEI and A β levels. Brain ILEI levels were selectively decreased in AD. CSF ILEI concentration correlated with that of A β and were reduced in AD and mild cognitive impairment.

Conclusion: ILEI and A β are released from distinct subpopulations of synaptic terminals in an activity-dependent manner, and ILEI negatively regulates A β production in specific synapse types. CSF ILEI might represent a surrogate marker for the accumulation of brain A β .

Keywords: Alzheimer's disease, amyloid- β , ILEI, neurotransmitter receptor, synapse

INTRODUCTION

Family with sequence similarity 3, member C (FAM3C) is a ubiquitously expressed, multi-functional secretory protein. It is upregulated by transforming growth factor β signaling and causes epithelial-mesenchymal transition of epithelial cells and hepatocytes; thus, FAM3C has also been named interleukin-like epithelial-mesenchymal transition inducer (ILEI) [1–5]. Other emerging functions of FAM3C/ILEI include inhibition of osteoblast differentiation and mineralization through Runx2 downregulation in the bone marrow [6, 7], and gluconeogenesis suppression via induction of heat shock factor 1, and activation of the phosphoinositide 3-kinase and Akt pathway in the liver [8, 9].

In previous studies, we found that extracellularly released ILEI interacts with the γ -secretase complex to suppress production of amyloid- β (A β) peptides [10]. A β is generated through β - and γ -secretase-mediated proteolytic processing of amyloid- β protein precursor (A β PP) and is released into the interstitial fluid (ISF) of brain parenchyma in a neuronal activity-dependent manner [11, 12]. Excessive accumulation of aggregated A β in the cerebral cortex and hippocampus is considered to initiate the pathogenic cascade of Alzheimer's disease (AD). Recent imaging studies revealed that A β deposition in the brain is tightly linked to baseline neuronal activity, and that component regions of the default mode network are the sites most vulnerable to A β deposition [13, 14]. ILEI reduces A β production by facilitating lysosome/proteasome-mediated turnover of the C-terminal fragments of A β PP while sparing γ -secretase activity. During AD pathogenesis, the expression of ILEI is significantly reduced in the brain and inversely correlated with accumulated A β levels [10, 15]. These findings suggest that reduced expression of brain ILEI is an antecedent event that prompts the inevitable A β pathology observed in AD.

We previously reported that ILEI colocalizes with A β PP and γ -secretase complex components at the presynaptic terminals [15]. However, two questions remain unanswered: 1) how is ILEI released into the ISF and 2) is there a relationship between extracellularly released ILEI and A β levels? In this study, we developed a sandwich ELISA for ILEI that enabled quantitative analysis of expression and secretion of ILEI in the mouse brain. Using *in vivo* microdialysis, we found that ILEI was released into the ISF in a neuronal activity-dependent manner, much like A β . Moreover, activation or inhibition of specific neurotransmitter receptors led to distinct changes in the extracellular levels of ILEI and A β in the cerebral cortex.

MATERIALS AND METHODS

Preparation of monoclonal antibodies against ILEI

To generate monoclonal antibodies against ILEI protein, two BDF1 mice were immunized with a recombinant His-tagged, secreted form of human ILEI (25–227 amino acid residues, #ATGP1251, ATGen Co. Ltd., Gyeonggi-do, Korea). After preparation of the lymph nodes and spleens, cells were fused with the myeloma cell line P3-X63-Ag8. The hybridoma supernatants of mixed clones were screened by ELISA. Among 95 clones that recognized the immunogen, three monoclonal antibody clones showed the highest immunoreactivity after the second round of subcloning by limiting dilution. Finally, two clones, namely 24C1 and 42C1, were selected by ELISA against recombinant mouse ILEI (R&D Systems Inc., Minneapolis, MN, Cat# 2868-FM). Both monoclonal antibodies were purified by protein A affinity chromatography from 1 L of each hybridoma cell culture supernatant. In addition, the antibody mAb24C1 was conjugated to horseradish

peroxidase according to the manufacturer's instructions (Dojindo, Kumamoto, Japan, Cat# LK11).

Development of a sandwich ELISA for ILEI

First, 96-well flat-bottom ELISA plates (Nunc, Thermo Fisher Scientific, Rochester, NY, Cat# 469914) were coated with mAb42C1 (144 ng/well in 100 μ L/well of 0.2 M sodium carbonate–bicarbonate buffer, pH 9.4). The plates were incubated at 4°C overnight and then washed three times with 300 μ L/well of PBS (pH 7.2) with 0.1% Tween 20. Nonspecific binding sites were blocked by incubation with a blocking reagent (IS-CD-500E; Cosmo Bio. Co, Ltd., Tokyo, Japan, Cat# IS-CD-500E) for 1 h at 37°C.

The standards were prepared with a solution of recombinant mouse ILEI (2868-FM; R&D system, Inc., Cat# 2868-FM) or human ILEI (15678-H08H-50, Sino Biological Inc., Beijing, China, Cat# 15678-H08H-50) in a dilution buffer (Immuno-Biological Laboratories Co, Ltd., Gunma, Japan, Cat# 27769D100). Standards of 0.313, 0.625, 1.25, 2.5, 5.0, and 10.0 ng/mL were prepared immediately before loading. Unknown samples were prepared in an appropriate dilution with dilution buffer. Wells were each loaded with 100 μ L of the designated solution. The plates were subsequently incubated for 18 h at 4°C without shaking before being washed five times.

The plates were then incubated with the detection antibody solution, which contained horseradish-peroxidase-conjugated antibody mAb24C1 at 50 ng/well in 100 μ L/well of a dilution buffer (Immuno Shot 2; Cosmo Bio, Cat# IS-002) for 1 h at 4°C. They were then washed five times, incubated for another hour at room temperature, and again washed five times. Subsequently, the plates were developed for 30 min with 100 μ L/well of a 3,3',5,5'-tetramethylbenzidine dihydrochloride substrate solution (ImmunoPure Turbo TMB; Pierce Chemical Co., Rockford, IL, Cat# 5120). The reaction was stopped by adding 100 μ L/well of 1 M sulfuric acid (Nacalai Tesque, Kyoto, Japan, Cat# 95626-06). Finally, the plates were read at a wavelength of 450 nm (Benchmark Plus; Bio-Rad Laboratories Inc., Hercules, CA, USA).

Immunoblotting

ILEI-knockout HEK293 cells [15] were transfected with expression plasmids using linear

polyethylenimine (Polysciences Inc., Warrington, PA, Cat# 23966). Cell lysates were sonicated on ice and centrifuged at 4°C and 15,000 rpm for 25 min. Per lane, 15–20 μ g of proteins were separated by 12% SDS-PAGE and transferred to a polyvinylidene fluoride membrane (Merck Millipore, Co., Billerica, MA, Cat# IPVH00010). These membranes were incubated with the primary antibodies at 4°C overnight before being washed and incubated with corresponding horseradish peroxidase-conjugated secondary antibodies (1:5,000, Merck Millipore, Cat# AP308P) for 1 h. This process was followed by enhanced chemiluminescence detection (Nacalai Tesque, Cat# 07880-70). Blots were scanned using a LAS-4000 imaging system (Fujifilm, Tokyo, Japan). The primary antibodies used were as follows: mAb42C1 (1:2,000), mAb24C1 (1:2,000), anti-GAPDH antibody (1:2,000, Merck Millipore, Cat# MAB2549), and anti-V5 antibody (1:2,000, Nacalai Tesque, Cat# 04434-94).

Animals

Four-month-old male C57BL/6J mice (CLEA Japan, Inc., Tokyo, Japan) and humanized mutant A β PP-knockin mice (*App*^{NL-G-F} mice [16]) were used in this study. Mice were maintained at room temperature (25°C) under a standard 12:12 h light:dark cycle, with food and water available *ad libitum*. *App*^{NL-G-F} mice were intraperitoneally injected with a mixture of anesthetics (Domitor, ZENOAQ, Fukushima, Japan; Vetorphale, Meiji Seika Pharma Co., Ltd., Tokyo, Japan; midazolam, Sando Co., Ltd., Tokyo, Japan) and then with an anti-anesthetic (Antisedan, ZENOAQ, Fukushima, Japan). Tetanus toxin (Sigma, St. Louis, MO, Cat# T3194) was also intraperitoneally administered. All experimental procedures were approved by the Institutional Animal Care and Use Committee of the Shiga University of Medical Science (Approval ID: 2018-12-1), and experiments were performed according to the Guide for the Care and Use of Laboratory Animals.

Measurement of ILEI and A β in the mouse brain

Mice were euthanized by cervical dislocation, and whole brains and cerebrospinal fluid (CSF) were obtained. Whole forebrains were homogenized using a motor-driven Teflon/glass homogenizer (10 strokes) in four volumes of Tris-buffered saline (50 mM Tris, pH 7.6, 150 mM NaCl, and 0.5 mM EDTA) that contained a protease inhibitor cocktail. The homogenates

were then centrifuged at 100,000 *g* for 20 min on a TLA 100.4 rotor in a TLX ultracentrifuge (Beckman, Palo Alto, CA, USA). The supernatants were taken as the soluble fractions and subjected to a protein assay (BioRad, Cat# 500-0116JA) and sandwich ELISAs specific for ILEI, mouse/rat A β 40 (Immuno-Biological Laboratories, Cat# 27720), or human total A β (Immuno-Biological Laboratories, Cat# 27729). Brain lysates were obtained by adding NP40 and CHAPSO to homogenates at 1% of each final concentration.

In vivo microdialysis

Microdialysis was performed as previously described by Takeda et al. [17]. Briefly, guide cannulas (8 mm in length) were stereotactically implanted into the right cerebral cortex (bregma 1.9 mm, 0.5 mm lateral to the midline, and 0.8 mm ventral to skull surface) of anesthetized mice, and then bonded in place with dental cement. Accordingly, the inserted dialysis probe was located in the medial prefrontal cortex spanning the anterior cingulate, prelimbic, and infralimbic areas, which are AD-vulnerable regions. At least two days after guide cannula implantation, a microdialysis probe with a 2 mm-long polyethylene membrane (1,000 kDa molecular weight cutoff, PEP-4-02, Eicom, Kyoto, Japan, Cat# 600132) was inserted through the guide, and the mouse was placed in a transparent acrylic cage (250×250×350 (height) mm). The probe was connected to peristaltic and microsyringe pumps with fluorinated ethylene propylene tubing (250 μ m in diameter): the syringe pump pushed and the peristaltic pump pulled a dialysis buffer (119 mM NaCl, 2.5 mM KCl, 2.5 mM CaCl₂, and 0.15% bovine serum albumin; filtered through a 0.22- μ m-pore-sized membrane) at a synchronous flow rate. After preperfusion with a dialysis buffer at a flow rate of 10 μ L/min for 2 h, dialyzed samples were collected into polypropylene tubes every 1 or 2 h using a fraction collector (EFC-96, Eicom). During sampling, flow rate was kept constant at 0.5 μ L/min. Sampling began at 16:00, and the mice were allowed to move freely in the cage while sampling occurred. The concentrations of ILEI and A β were measured using the ELISAs described above. Basal levels of ILEI or A β were defined as the mean concentration from four samples obtained before reverse dialysis. All values for each mouse were then normalized as percentages of the basal level for each point.

Assessment of mouse locomotor activity

To assess mouse locomotor activity during microdialysis, we used the Scanet MV-40 system (Melquest, Toyama, Japan). Vertical and horizontal movements of mice were tracked and measured every 60 min for 2 days using digital counters with infrared sensors, which were crosswise distributed at 6-mm intervals and a height of 30 mm above the floor of a transparent acrylic cage (250×250 mm). The moving distances of mice every hour were expressed in arbitrary units.

Reverse microdialysis

The following compounds were used for reverse microdialysis: tetrodotoxin (Fujifilm Wako, Tokyo, Japan, Cat# 206-11071), AMPA (Abcam, Cambridge, UK, Cat# ab12005), NBQX disodium salt (Abcam, Cat# ab144489), NMDA (Nacalai Tesque, Cat# 22034-16), D-AP5 (Abcam, Cat# ab120003), diazepam (Fujifilm Wako, Cat# 045-18901), picrotoxin (Sigma Chemicals, Cat# P1675), (R, S)-Baclofen (Abcam, Cat# ab120149), CGP55845 hydrochloride (Sigma Chemicals, Cat# SML0594), nicotine (Nacalai Tesque, Cat# 24332-62), D-tubocurarine chloride (Nacalai Tesque, Cat# 35637-84), pilocarpine hydrochloride (Nacalai Tesque, Cat# 28008-31), and atropine sulfate (Nacalai Tesque, Cat# 03533-11). For reverse microdialysis, compounds were diluted at the indicated concentration in Ringer's solution.

Autopsied human brain tissues

Frozen brain tissues from the temporal cortex of 15 deceased patients with AD, 15 age-matched non-neurological disease control subjects, and 10 non-AD neurological disease control subjects were obtained from the Brain Bank for Aging Research, Tokyo Metropolitan Institute of Gerontology (Tokyo, Japan). All study subjects or their next of kin provided written informed consent for brain donation, and experimental procedures were approved by the Shiga University of Medical Science Review Board (Approval ID: 28-096). All patients with AD fulfilled the National Institute of Neurological and Communicative Disorders and Stroke-Alzheimer's Disease and Related Disorders Associations criteria for probable AD. Soluble fractions of temporal cortex homogenates were prepared as previously described [10].

Clinical CSF samples

CSF was analyzed in control subjects (mean age 76.88 years, $n=25$), MCI subjects (mean age 71.24 years, $n=25$), and patients with AD (mean age 75.84 years, $n=25$). Written informed consent was obtained from each participant before lumbar puncture for CSF collection. CSF analysis was approved by the Ethics Committees of Niigata University (Approval ID: 2015-2427). CSF concentrations of A β 38, A β 40, and A β 42 were analyzed using V-PLEX A β Peptide Panel 1 (6E10) (Meso Scale Discovery, Rockville, MD) with MESO QuickPlex SQ 120 (Meso Scale Diagnostics). Intra- and inter-assay coefficients of variation were $<20\%$ for all assays. The ILEI measurement of CSF samples was approved by the Ethics Committees of Shiga University of Medical Science (Approval ID: 27-210).

Statistical analysis

Statistical analyses involved two-tailed unpaired Student's t -tests or one-way ANOVA combined with Dunnett's test for multiple comparisons. Correlation analyses were performed using the Spearman's rank correlation test. StatPlus:mac LE software (Analyst-Soft, Vancouver, Canada) was used for statistical analyses. All data are presented as means \pm SEMs. p values <0.05 were considered to be statistically significant.

RESULTS

Monoclonal antibodies 24C1 and 42C1 recognize distinct epitopes of ILEI protein

We generated monoclonal antibodies against ILEI by immunizing BDF1 mice with recombinant His-tagged, human ILEI that was purified from conditioned medium of ILEI-overexpressing HEK293 cells. Based on immunoblotting of HEK293 cell lysate and ELISA against recombinant ILEI, we selected the clones 24C1 and 42C1. The monoclonal antibodies mAb24C1 and mAb42C1 recognized both human and mouse ILEI proteins according to immunoblotting and ELISA.

To define each epitope of these antibodies, we first generated expression vectors for human ILEI mutants harboring deletion or truncation of amino acid residues 25–99 (Δ 25–99), 100–154 (Δ 100–154), 155–190 (Δ 155–190), or 191–227 (Δ 191–227) (Fig. 1A). Immunoblotting of mutant ILEI-transfected HEK293 cell lysates revealed that mAb24C1

failed to label ILEI- Δ 155–190, whereas mAb42C1 did not react with ILEI- Δ 191–227 (Fig. 1B). We also prepared several missense ILEI mutants harboring alanine substitutions of evolutionally conserved amino acid residues: G103A, G169A, D151A, R179A, W212A, C58A, C64A, C86A, and C221A. Immunoblotting revealed that mAb24C1 and mAb42C1 selectively lacked immunoreactivity to G169A-ILEI and W212A-ILEI, respectively (Fig. 1C). According to a previous report on crystal structure [18], Gly¹⁶⁹ and Trp²¹² are surface-exposed and distant from each other in their respective locations (Fig. 1D). These results suggest that mAb24C1 and mAb42C1 recognize distinct epitopes of ILEI, to which the residues Gly¹⁶⁹ and Trp²¹² are critical, respectively.

Development and validation of the ILEI-specific ELISA

In our sandwich ELISA that was specific for ILEI, mAb42C1 was suitable as a capture antibody and horseradish peroxidase-labeled mAb24C1 was useful as a detection antibody. The optimized concentrations of the capture and detection antibodies were 1.44 and 0.50 μ g/mL, respectively. The performance of this ELISA for recombinant mouse and human ILEI are shown in Fig. 1E. The standard curves were based on six serial dilutions of mouse or human recombinant ILEI and were linear over 0.31–10.0 ng/mL. The detection limit (3.3 s/a, where s = SD of the blank; a = slope of the standard curve) and the quantification limit (10 s/a), which were based on eight independent determinations of a blank in standard solutions, were 0.04 and 0.11 ng/mL for mouse ILEI, respectively, and 0.05 and 0.16 ng/mL for human ILEI, respectively.

For validation of the assay at different dilutions, we used soluble fractions of mouse brain homogenates diluted at 1:10. Dilutional parallelism was determined by evaluating each sample at its initial strength (1:10) and at dilutions of 1:2, 1:4, and 1:8. Observed-to-expected ratios for the dilutional parallelism of each sample of the full-strength solution ranged from 85% to 136%. Spiking recovery was determined by adding 0.0, 1.25, 2.50, and 5.00 ng/mL of recombinant ILEI to mouse brain homogenate samples. Observed-to-expected ratios for spiking recovery of the homogenate diluted at 1:40 ranged from 88% to 89%. The intra-assay coefficient of variation for soluble fractions of brain homogenates was $<10\%$.

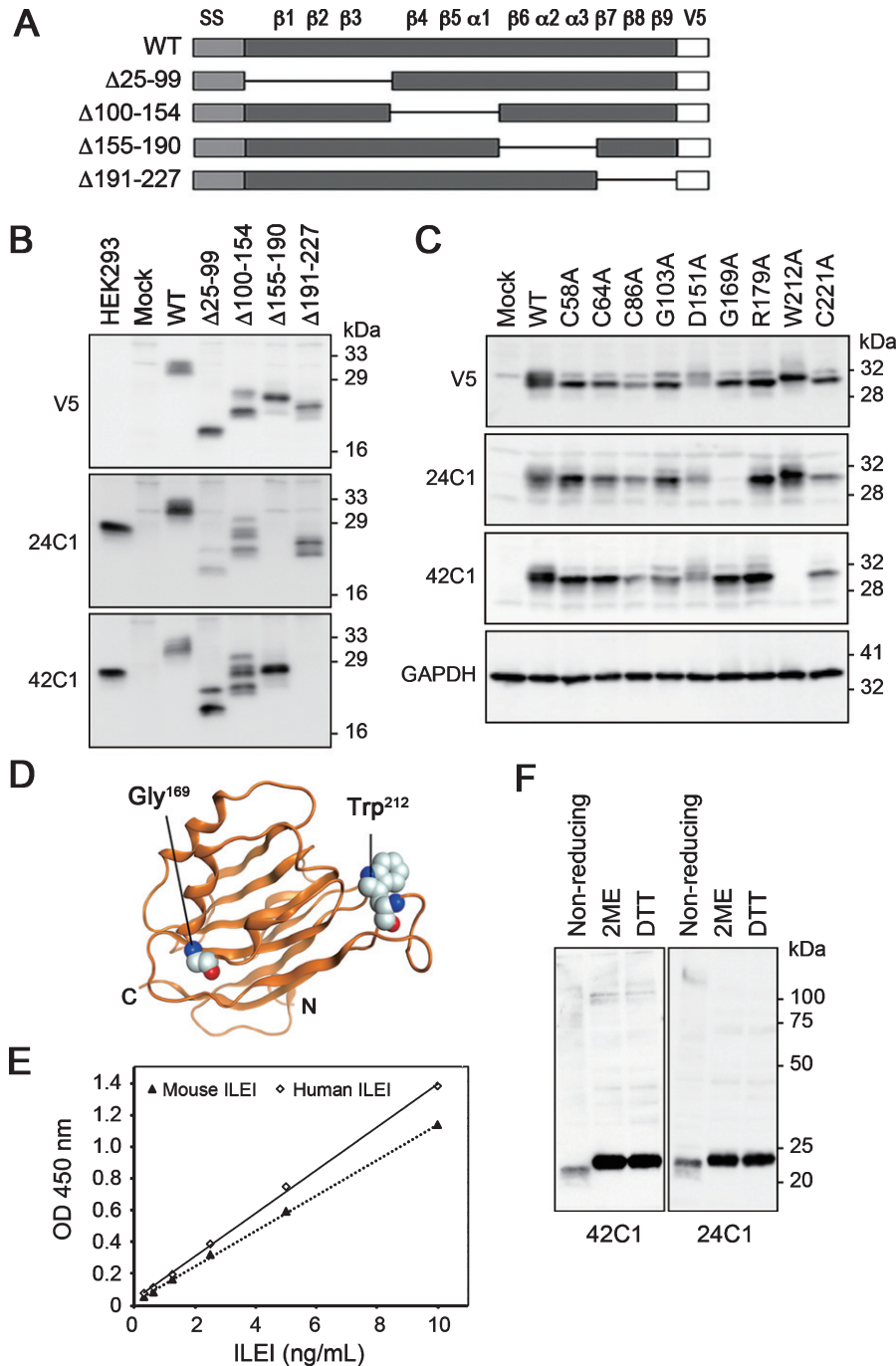


Fig. 1. Characterization of mAb24C1, mAb42C1, and sandwich ELISA for ILEI. A) Scheme of the ILEI construct and deletion mutants. The predicted conformation model of ILEI protein contains nine β -sheets (β) and three α -helices (α). SS, signal sequence; V5, V5 tag. B) Lysates of HEK293 cells (lane 1) or ILEI-knockout HEK293 cells transiently transfected with mock, V5-tagged wild-type, or various ILEI deletion mutants (lanes 2–7) were subjected to SDS-PAGE. Blots were probed with anti-V5 antibody, mAb24C1, or mAb42C1. C) Immunoblotting using lysates of ILEI-knockout HEK293 cells transiently transfected with mock, V5-tagged wild-type, or various missense mutant ILEI constructs. Blots were probed with anti-V5, mAb24C1, mAb42C1, or anti-GAPDH antibodies. D) Gly¹⁶⁹ and Trp²¹² are distant from each other on the ILEI structure: Gly¹⁶⁹ is located in the loop between the 2nd and 3rd α -helices, whereas Trp²¹² is located in the loop between the 8th and 9th β -sheets. E) Representative standard curves from ELISA for human and mouse ILEI proteins. F) Immunoblotting of mouse brain lysate samples with no reducing agent (nonreducing), 5% 2-mercaptoethanol (2ME), or 75 mM dithiothreitol (DTT). Blots were probed using mAb24C1 or mAb42C1.

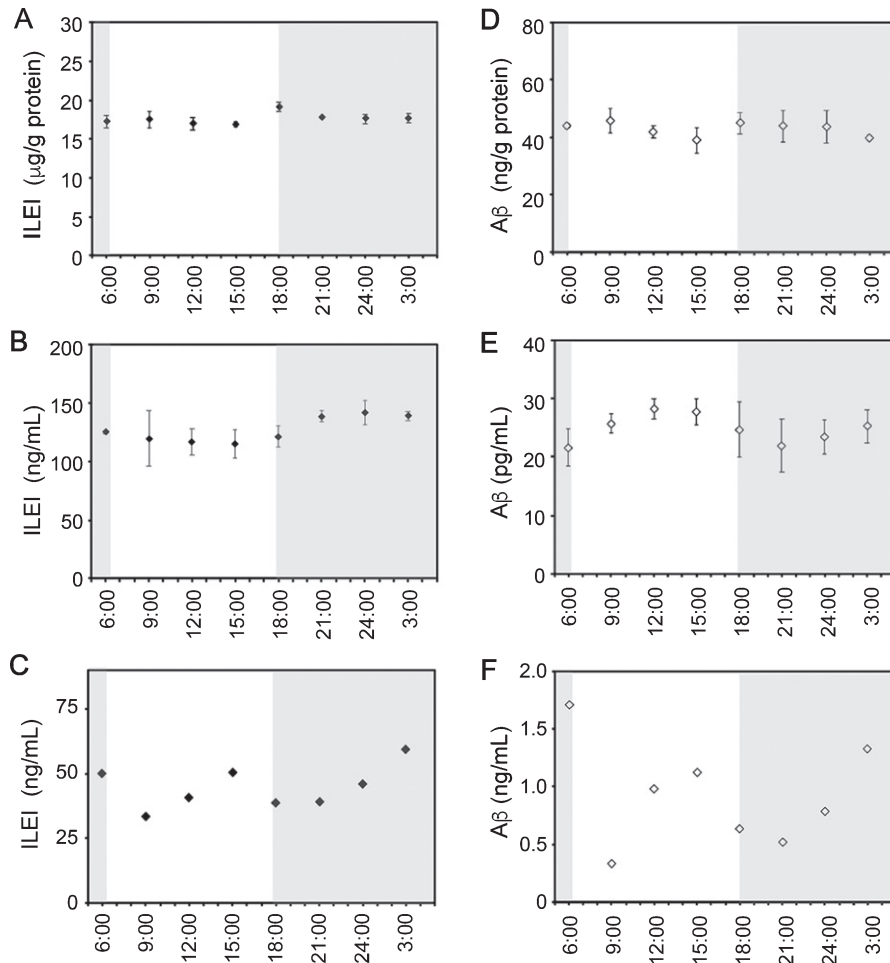


Fig. 2. Extracellular levels of ILEI periodically fluctuate in the mouse brain. Brains and cerebrospinal fluid (CSF) were obtained every 3 h from C57BL/6J mice that were housed under a 12:12 h light:dark cycle. CSF samples from three mice at each time point were combined. ILEI levels in brain lysates (A), the soluble fractions of brains (B), and CSF (C) were measured using ELISA. A β levels in brain lysates (D), the soluble fractions of brains (E), and CSF (F) were also measured using mouse A β 40-specific ELISA. Values are shown as means \pm SEMs ($n = 3$).

A study reported homodimerization of ILEI via intermolecular disulfide bonds [18]. According to the predicted conformation of dimerized ILEI [18], mAb42C1 recognized the opposite side of the binding interface, whereas the recognition site of mAb24C1 may be occluded by the binding interface. Both antibodies detected a single band corresponding to monomer ILEI in mouse brain lysates under reducing or nonreducing conditions (Fig. 1F). The nonreduced ILEI monomer migrated faster in SDS-PAGE than the disulfide-reduced ILEI monomer (Fig. 1F), which can be explained by the formation of intramolecular disulfide bonds [18]. This indicated that no detectable level of ILEI homodimer was present in the mouse brain, at least using these antibodies.

Expression and secretion of ILEI in the mouse forebrain

We collected brains and CSF every 3 h for 24 h from C57BL/6J mice housed under a 12:12 h light:dark cycle and then measured ILEI levels using the established ELISA. To examine expression levels of brain ILEI, we prepared NP40- and CHAPSO-solubilized lysates of forebrains. ILEI concentrations of forebrain lysates were within a relatively narrow range during day/night cycles (Fig. 2A). To assess secretion of ILEI, we used the supernatant from ultracentrifuged forebrain homogenates. The ILEI concentrations of the soluble fractions changed periodically (Fig. 2B); thus, the extracellular release of

ILEI apparently fluctuated over time. The levels of CSF ILEI also fluctuated but were not synchronized with levels of ILEI in the soluble brain fractions (Fig. 2C).

Furthermore, we measured A β concentrations in these same samples. A β levels showed fluctuations that were more prominent in the soluble fractions than in the lysates and were not associated with the fluctuations of ILEI levels (Fig. 2D, E). However, A β fluctuation was roughly parallel to ILEI fluctuation in the CSF (Fig. 2F).

Monitoring of cortical ISF ILEI and A β by in vivo microdialysis

We used *in vivo* microdialysis to monitor ISF ILEI and A β in the cerebral cortex of conscious, freely-moving *App^{NL-G-F}* knockin (KI) mice (3–4 months old), in which the humanized mutant A β PP is expressed under its endogenous promoter [16]. Dialysates were collected every hour and mouse movement was tracked. Levels of ISF ILEI periodically fluctuated and higher levels were weakly associated with higher locomotor activity (Fig. 3A, B). Intraperitoneally injected anesthetics suppressed ILEI levels in the dialysates; however, these levels were restored by treatment with an anti-anesthetic (Fig. 3C). Anesthetic treatment also decreased A β levels with kinetics that were similar to ILEI levels (Fig. 3D). Although ISF A β levels have previously been reported to fluctuate over time [19], we found that ISF ILEI levels tended to inversely fluctuate relative to the fluctuating levels of A β (Fig. 3E, F).

Activity-dependent release of ILEI and A β

Using reverse microdialysis, we tested pharmacological modulation of synaptic activity. Preliminary reverse microdialysis of bromophenol blue solution in the frontal cortex resulted in its focal diffusion within the restricted area even after continuous perfusion for 48 h (Fig. 4A). Perfusion with tetrodotoxin, a voltage-dependent sodium channel blocker, suppressed ILEI levels in a dose-dependent manner (Fig. 4B). A similar decrease in ISF A β levels was reported in a previous report [12]. Intraperitoneal administration of tetanus toxin, an inhibitor of synaptic vesicle exocytosis, decreased ILEI and A β levels in the dialysates (Fig. 4C), indicating that the release of ILEI and A β into the ISF is associated with synaptic vesicle exocytosis. Levels of ISF ILEI decreased by >95% after tetanus toxin treatment, suggesting

that ISF ILEI was predominantly derived from synaptic vesicles. Furthermore, given that the rates of ILEI and A β showed similar declines after tetanus toxin treatment, the half-life of ISF ILEI was apparently equivalent to that of A β , which has previously been reported to be as short as ~ 2 h [20].

Activation and inhibition of glutamatergic receptors

Our finding that ISF levels of ILEI and A β were similarly associated with neuronal activity but inversely fluctuated in untreated mice seemed paradoxical. To address this issue, we examined how evoked activation or basal activity inhibition of distinct neurotransmitter receptors affected ISF ILEI and A β levels. Hettinger et al. [21] reported that reverse dialysis of AMPA and NBQX, an agonist and antagonist of AMPA-type receptors, respectively, gradually decreased ISF A β levels in the hippocampus of mutant A β PP- and mutant Presenilin-1-double transgenic (*APP^{swe}/PS1 Δ E9*) mice. We observed similar effects of AMPA and NBQX on ISF A β levels following cortical microdialysis in *App^{NL-G-F}* mice (Fig. 5A, B). Specifically, NBQX decreased ISF ILEI levels, whereas AMPA increased ISF ILEI levels from 20 h after reverse dialysis began (Fig. 5A, B). An important characteristic of AMPA receptors is rapid desensitization; in a previous study, perfusion of 1 μ M and 100 μ M AMPA into the rat hippocampus increased and decreased the 5-HT level in dialysates, respectively [22]. Similarly, we tested perfusions of 1, 20, and 100 μ M AMPA and found that ILEI levels increased in a dose-dependent manner (Fig. 5C); this suggests that desensitization of AMPA receptors did not affect ILEI release. Hettinger et al. (2018) reported a similar result for A β release [21].

Treatment with higher doses of NMDA reduced ISF A β in the neocortex of *App^{NL-G-F}* mice whereas treatment with D-AP5, an NMDA receptor antagonist, markedly increased ISF A β levels (Fig. 5D), consistent with previous findings from hippocampal microdialysis of *APP^{swe}/PS1 Δ E9* transgenic mice [23]. Similarly, NMDA reduced ISF ILEI levels; however, D-AP5 treatment led to a delayed decrease in ILEI levels (Fig. 5E).

Activation and inhibition of GABAergic receptors

Microdialysis perfusion of diazepam and baclofen, agonists of GABA_A and GABA_B receptors, respectively, suppressed ISF ILEI and A β levels, whereas

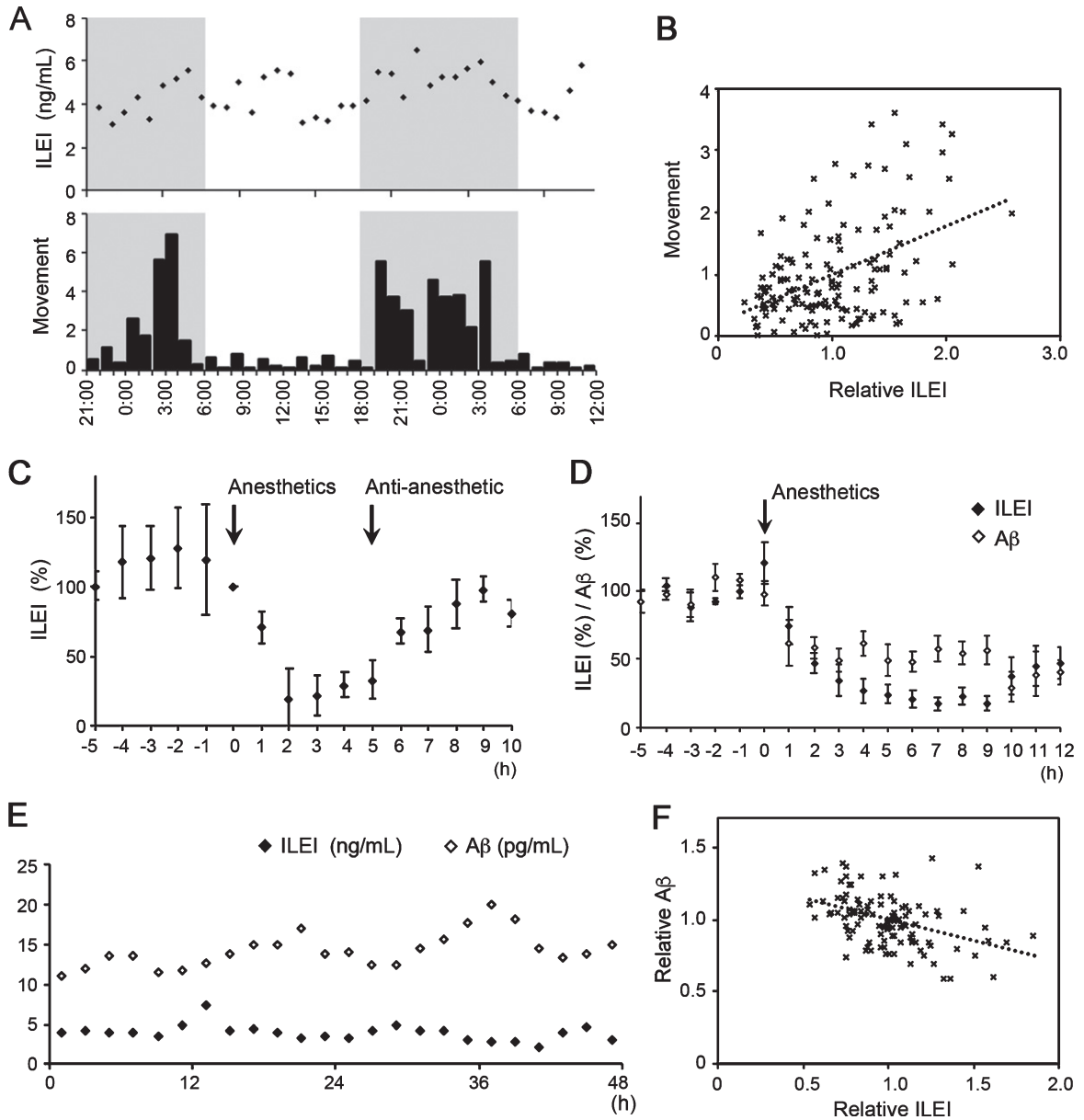


Fig. 3. ISF ILEI levels are positively correlated with locomotor activity but inversely associated with ISF A β levels. A) Cerebrocortical ILEI levels were monitored using *in vivo* microdialysis in a C57BL/6J mouse; the movement distance of these mice was also recorded (distances moved per hour are expressed in arbitrary units). A representative result is shown. B) Graph showing the correlation between ISF ILEI levels and movement distance ($n = 144$, $r = 0.460$). C) Mice were intraperitoneally injected with anesthetics and then with anti-anesthetic during monitoring of ISF ILEI. Values are shown as means \pm SEMs from three independent experiments. D) Cerebrocortical ISF levels of ILEI and A β were measured after intraperitoneal injection with anesthetics. Values shown represent means \pm SEMs from three independent experiments. All values for each mouse were normalized as percentages of the basal level, which was defined as the mean concentration from samples obtained before injection (C, D). E) Cortical ISF levels of ILEI and A β were simultaneously monitored via *in vivo* microdialysis in *App^{NL-G-F}* mice for 2 days. A representative result is shown. F) Reverse correlation between ISF ILEI and A β levels ($n = 112$, $r = 0.423$).

perfusion of the antagonists of these receptors led to a marked increase in both ILEI and A β levels (Fig. 6). These results are consistent with the sustained stimulation of GABAergic receptors suppressing overall

cortical neuronal activity. It must be noted, however, that the decrease in ISF ILEI levels after diazepam treatment was rapid and reached $>90\%$ at its peak, while ISF A β levels decreased to $<50\%$ of the

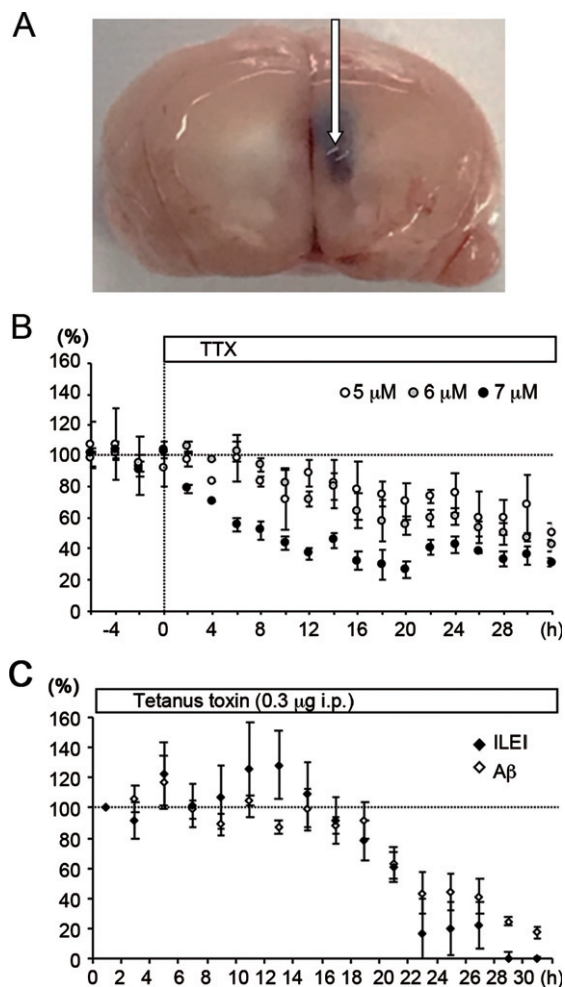


Fig. 4. ILEI is released into the ISF in a synaptic activity-dependent manner. A) Reverse microdialysis of bromophenol blue for 48 h resulted in local diffusion in the frontal cortex of mice. The arrow indicates the position of the microdialysis probe. B) Reverse microdialysis with tetrodotoxin (TTX) reduced the cortical ISF ILEI levels of *App^{NL-G-F}* mice in a dose-dependent manner. C) Intraperitoneal administration of tetanus toxin decreased ISF levels of ILEI and A β in dialysates. Values are shown as means \pm SEMs from three independent experiments. All values for each mouse were normalized as percentages of the basal level, which was defined as the mean concentration from samples obtained before reverse dialysis or treatment.

baseline. These findings suggest that ILEI may be released directly from GABA_A receptor-expressing neurons at their depolarization. During the perfusion, we did not observe any obvious changes in mouse behavior or awake-sleep cycles.

Activation and inhibition of cholinergic receptors

Perfusion of nicotine and tubocurarine, an agonist and antagonist of nicotinic acetylcholine (ACh)

receptors, respectively, increased ISF A β levels (Fig. 7A, B). Although nicotine treatment did not alter the average levels of ISF ILEI, it did result in a higher amplitude and more regular cycle of periodic fluctuations in these levels: the amplitude was approximately 50% that of the baseline level over a \sim 12 h cycle (Fig. 7A). Tubocurarine treatment did not have any clear effect on ISF ILEI in the acute phase but increased ILEI levels $>$ 24 h after perfusion began (Fig. 7B). Perfusion of pilocarpine and atropine, an agonist and antagonist for muscarinic ACh receptors, respectively, decreased and increased ISF A β levels, respectively (Fig. 7C, D), consistent with previous findings [24, 25]. Similarly, pilocarpine decreased ILEI levels; however, atropine did not affect ILEI levels (Fig. 7C, D).

Reduced expression of ILEI in AD brains

Using semi-quantitative immunoblotting, we previously showed that ILEI expression levels decreased in autopsy brains of AD patients compared with those of non-demented controls and non-AD disease controls, including brains of patients with corticobasal degeneration, progressive supranuclear palsy, amyotrophic lateral sclerosis, Parkinson's disease, and dementia with Lewy bodies [10]. To measure ILEI levels in autopsied brains, we validated our ELISA method with a soluble fraction of human brains as previously described. The limits of detection and quantification were 0.24 and 0.74 ng/mL, respectively. The observed-to-expected ratios of the dilutional parallelism and spiking recovery were in the ranges of 94%–99%, and 72%–99%, respectively. The intra-assay coefficient of variation was $<$ 10%. Using ELISA, we examined ILEI levels in the same set of autopsied brains according to our previous report [10] and confirmed a significant and selective decrease in ILEI levels in AD brains (Fig. 8A). Furthermore, we measured ILEI concentrations in CSF samples of clinical subjects and found that CSF ILEI levels correlated with those of A β 40 and A β 42 and were lower in AD and MCI patients than in control patients (Fig. 8B, C).

DISCUSSION

We quantitatively examined the extracellular release of ILEI protein in the medial prefrontal cortex of the mouse brain while also comparing ILEI levels with those of A β peptides. We found that ISF ILEI levels exhibited circadian fluctuation, which

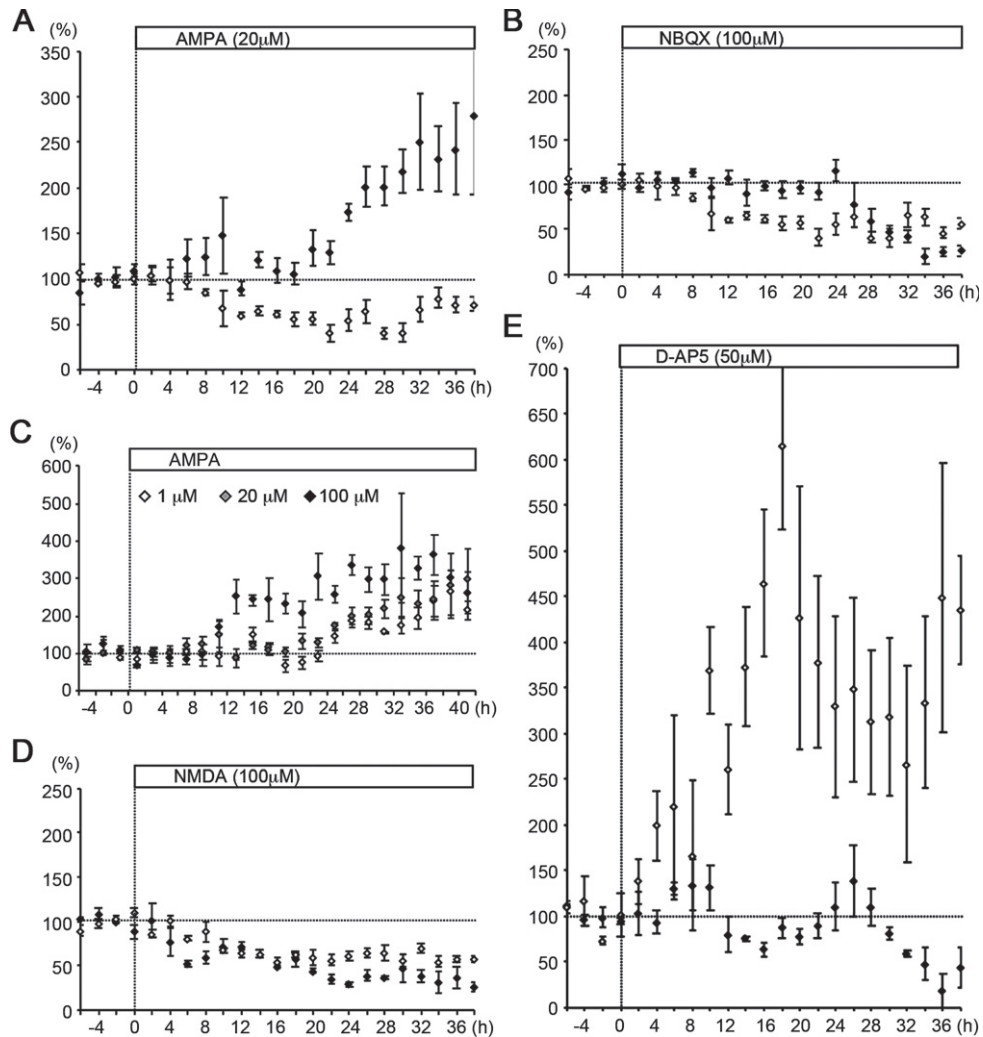


Fig. 5. Extracellular ILEI and A β levels were differentially altered by treatment with agonists or antagonists of AMPA and NMDA receptors. Indicated doses of AMPA (A), NBQX (B), AMPA (C), NMDA (D), and D-AP5 (E) were administered through reverse microdialysis to the frontal cortex of *App^{NL-G-F}* mice. The graphs show relative levels of extracellular ILEI (closed diamonds) and A β (open diamonds). Values are shown as means \pm SEMs from three independent experiments. All values for each mouse were normalized as percentages of the basal level, which was defined as the mean concentration from samples obtained before reverse dialysis.

was similar to reports on A β . Our results suggested that extracellular release of these proteins was associated with neuronal activity and largely depended on tetanus toxin-sensitive exocytosis of the synaptic vesicle and the circadian fluctuation of ILEI and A β was loosely linked to mouse locomotor activity. In addition, we revealed a superimposed fluctuation in which ILEI and A β levels were inversely altered. Perfusion of agonists or antagonists for glutamate, GABA, and ACh receptors differentially altered ISF ILEI and A β levels, indicating that these proteins are released from distinct subpopulations of presynaptic terminals. Declines in ISF ILEI and A β

levels followed inhibited depolarization of AMPA, GABA_A, or GABA_B receptor-expressing neurons, which suggests that the normal activities of these receptors directly or indirectly sustain ISF ILEI and A β levels *in vivo*.

The cerebral cortex predominantly consists of two types of neurons: 1) glutamatergic projection neurons reciprocally connected to the thalamus and to each other, and 2) mainly local circuit GABAergic neurons [26]. The basal forebrain cholinergic system innervates the neocortex to act as a slow modulator that increases the excitability of neuronal networks [27]. In the present study, reverse microdialysis in

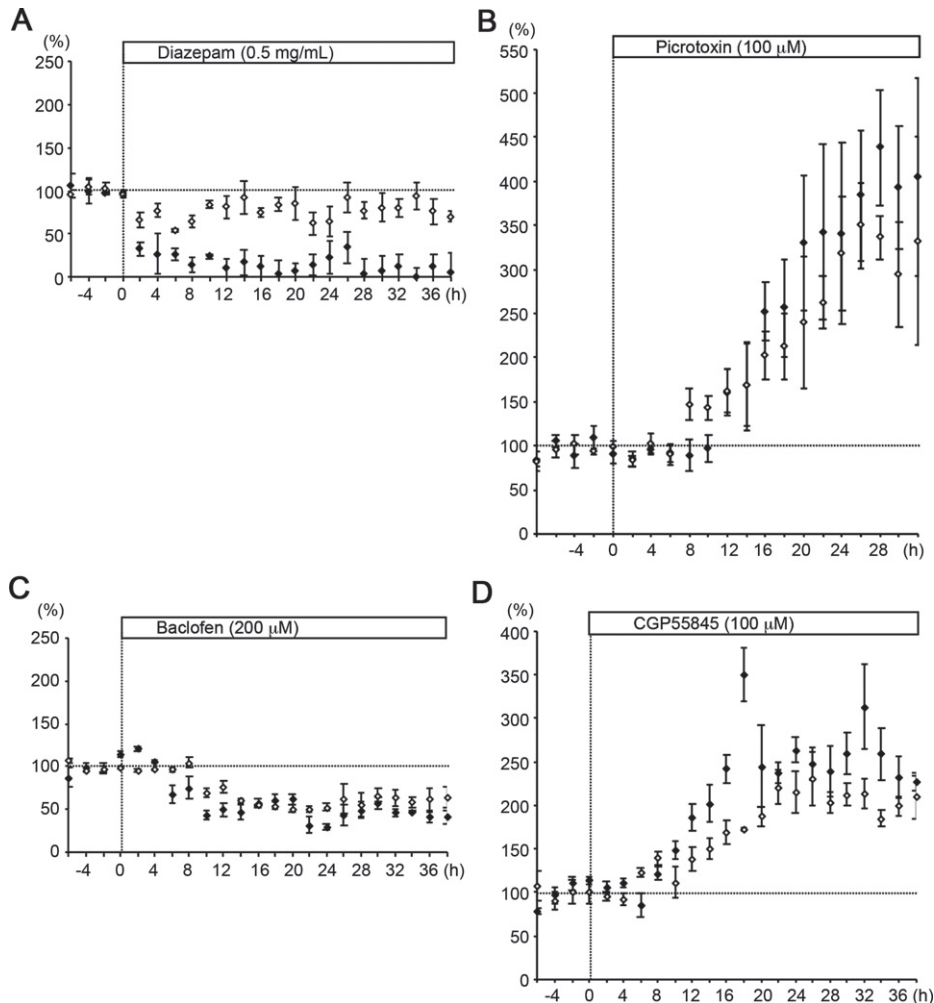


Fig. 6. Activation of GABA_A or GABA_B receptors reduced extracellular ILEI and A β levels. Indicated doses of diazepam (A), picrotoxin (B), baclofen (C), and CGP55845 (D) were administered through reverse microdialysis to the frontal cortex of *App*^{NL-G-F} mice. The graphs show relative levels of extracellular ILEI (closed diamonds) and A β (open diamonds). Values are shown as means \pm SEMs from three independent experiments. All values for each mouse were normalized as percentages of the basal level, which was defined as the mean concentration from samples obtained before reverse dialysis.

the cerebral cortex resulted in focal diffusion of compounds even after prolonged perfusion, and infusion of agonists or antagonists was presumed to modulate activation of the target receptor-expressing neurons near the dialysis probe. Output synapses of the local circuit neurons are located near the dialysis probe, whereas axon terminals of the projection neurons are far from the probe but involved in the reciprocal networks. ILEI and A β are known to be released predominantly from presynaptic terminals [28, 29]. Hence, prolonged perfusion of receptor modulators would likely have both direct and indirect effects on the ISF ILEI and A β levels around the probe. Such indirect effects are predicted to be mediated by

the inter-regional network connections in which the probe-inserted site is involved. Nevertheless, reverse microdialysis with receptor modulators in the cerebral cortex resulted in similar effects on ISF A β levels as those previously reported in the hippocampus [21, 23].

AMPA receptors are expressed on the major population of synapses that mediate fast excitatory transmission in the cerebral cortex. Among the receptor modulator treatments tested in this study, AMPA treatment was unique in producing opposing effects on ISF ILEI and A β levels: an increase in ILEI and a decrease in A β . The paradoxical finding that the levels of ILEI and A β in the ISF are similarly associated

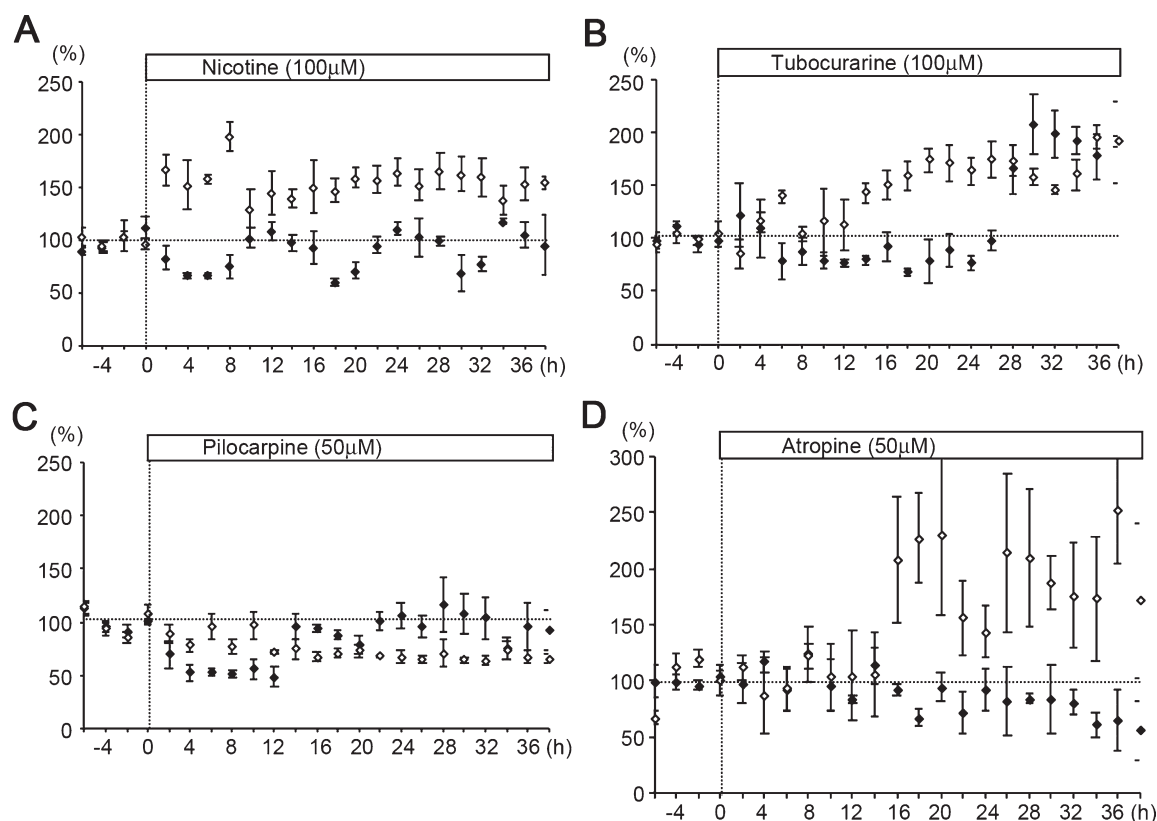


Fig. 7. Extracellular ILEI and A β levels were differentially altered by treatment with agonists or antagonists of nicotinic and muscarinic ACh receptors. Indicated doses of nicotine (A), tubocurarine (B), pilocarpine (C), and atropine (D) were administered through reverse microdialysis to the frontal cortex of *App^{NL-G-F}* mice. The graphs show relative levels of extracellular ILEI (closed diamonds) and A β (open diamonds). Values are shown as means \pm SEMs from three independent experiments. All values for each mouse were normalized as percentages of the basal level, which was defined as the mean concentration from samples obtained before reverse dialysis.

with neuronal activity but fluctuate inversely can possibly be explained by a transition in the dominance of AMPA receptor-mediated synaptic activation. On the other hand, continuous stimulation of nicotinic ACh receptors enhanced the spontaneous fluctuation of ISF ILEI levels: nicotine treatment resulted in a higher amplitude and more regular cycle of periodic fluctuations in ILEI levels. Nicotinic cholinergic stimulation is known to potentiate glutamatergic transmission [30] and is required for the generation of synchronized ultraslow fluctuation of neuronal activity in the prefrontal cortex [31]. However, the underlying mechanism of these effects could not be addressed in the present study and it will therefore require further investigation in future research.

Recently, Rice et al. [32] reported that the distribution of A β PP is prominent in GABAergic interneurons in the hippocampus, and they showed that 98% of A β PP-positive cells in the CA1 region

are GABA $_B$ receptor subunit 1-positive. In the present study, treatment with agonists of GABA $_A$ or GABA $_B$ receptors reduced ISF A β levels whereas treatment with antagonists of these receptors remarkably increased ISF A β levels. While our results seem to be discordant with the findings of [32], it is currently unclear whether this discrepancy is due to differences between the hippocampus and cerebral cortex or between direct and indirect effects.

Cholinergic receptors are expressed at only 3% of the total number of nerve terminals in the rat hippocampus, and A β PP is then colocalized at approximately 3%–4% of cholinergic terminals [33]. Nevertheless, in our study, prolonged perfusion of agonists or antagonists of these receptors led to marked changes in cortical ISF levels of ILEI and A β . For example, nicotine perfusion unexpectedly enhanced ISF A β levels in the cerebral neocortex. Chronic nicotine treatment has been shown to reduce

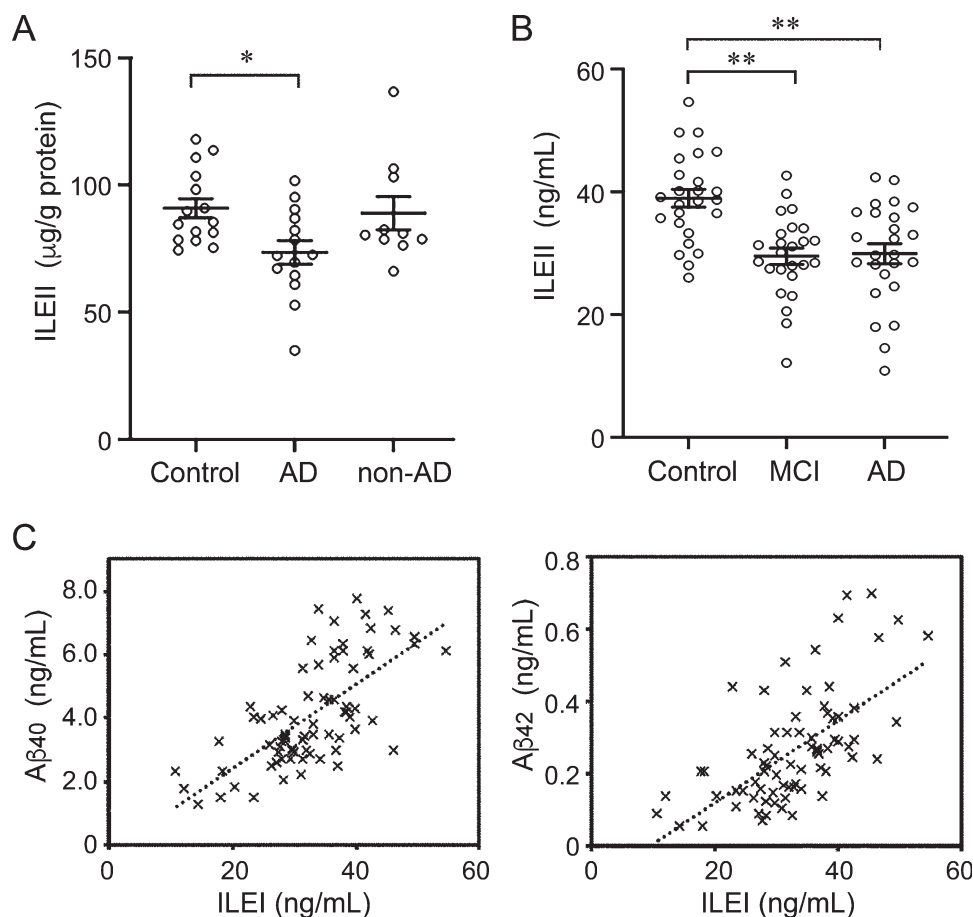


Fig. 8. Reduced expression of ILEI in the AD brain. A) ILEI levels in soluble fractions from temporal cortex homogenates from AD brains ($n = 15$), age-matched non-neurological disease controls ($n = 15$), and non-AD neurological disease controls ($n = 10$) were measured using ELISA. Non-AD disease controls included corticobasal degeneration (2 cases), progressive supranuclear palsy (2 cases), amyotrophic lateral sclerosis (2 cases), Parkinson's disease (2 cases), and dementia with Lewy bodies (2 cases). Lines and error bars represent means \pm SEMs. Statistical analysis was performed using Dunnett's multiple comparison test. Significant differences relative to the ratio in controls are indicated (* $p < 0.05$). B) ILEI concentrations in CSF from AD patients ($n = 25$), MCI patients ($n = 25$), and age-matched non-neurological disease controls ($n = 25$) were measured using ELISA. Lines and error bars represent means \pm SEMs. Statistical analysis was performed using Dunnett's multiple comparison test. Significant differences relative to the ratio in controls are indicated (** $p < 0.01$). C) CSF ILEI concentrations were correlated with those of A β 40 ($n = 75$, $r = 0.678$) and A β 42 ($n = 75$, $r = 0.627$).

A β deposition in the brain of A β PP-transgenic (Tg2576) mice [34]. These findings suggest the possibility that nicotine could produce unidentified effects on A β degradation or aggregation. Indeed, cotinine, a stable metabolite of nicotine, can inhibit A β oligomerization and fibrillation [35].

The results of this study are consistent with those of previous studies showing that ILEI and A β PP are constituents of the release-competent pool of synaptic vesicles [15, 36]. Although the modulatory activities of released A β on synaptic transmission have been reported (reviewed by [37]), the physiological functions of ILEI at the synaptic terminal remain to be

clarified. Barthet et al. [38] reported that inhibiting γ -secretase cleavage of synaptic A β PP impairs the replenishment of release-competent synaptic vesicles, thus, extracellular ILEI might modify these functions of A β and A β PP.

In contrast to ISF levels of ILEI and A β , CSF levels of these proteins were roughly paralleled in mouse and clinical samples. The difference in these fluctuations between ISF and CSF may be attributable to differences in fluid volume between ISF and CSF or in turnover dynamics between ILEI and A β . Our finding that CSF ILEI levels were significantly lower in AD and MCI patients than in control patients

suggests that CSF ILEI might be a surrogate marker for brain A β accumulation or AD development. To more accurately evaluate A β and ILEI levels in clinical samples, it will, however, be necessary to carefully assess the condition of patients before and during CSF sampling.

ACKNOWLEDGMENTS

This research was supported by AMED under Grant Number 20dm0107141h0004 (to MNI), 20dm0107142h0004 (to TS), 20dm0107143h0004 (to TI), JP20dm0207073 (to TI), and JP18dm0107103 (to SM). This work was also supported in part by Grants-in-Aid for Scientific Research from the Ministry of Education, Culture, Sports, Science, and Technology, Japan (19K16912 to MNa, 19H03546 to MNI, and 19K21585 to MNI), and Smoking Research Foundation (to MNI).

Authors' disclosures available online (<https://www.j-alz.com/manuscript-disclosures/20-1174r1>).

REFERENCES

- [1] Chaudhury A, Hussey GS, Ray PS, Jin G, Fox PL, Howe PH (2010) TGF- β -mediated phosphorylation of hnRNP E1 induces EMT via transcript-selective translational induction of Dab2 and ILEI. *Nat Cell Biol* **12**, 286-293.
- [2] Lahsnig C, Mikula M, Petz M, Zulehner G, Schneller D, van Zijl F, Huber H, Csiszar A, Beug H, Mikulits W (2009) ILEI requires oncogenic Ras for the epithelial to mesenchymal transition of hepatocytes and liver carcinoma progression. *Oncogene* **28**, 638-650.
- [3] Mackenzie NC, Raz E (2006) Found in translation: A new player in EMT. *Dev Cell* **11**, 434-436.
- [4] Mauri P, Scarpa A, Nascimbeni AC, Benazzi L, Parmagnani E, Mafficini A, Della Peruta M, Bassi C, Miyazaki K, Sorio C (2005) Identification of proteins released by pancreatic cancer cells by multidimensional protein identification technology: A strategy for identification of novel cancer markers. *FASEB J* **19**, 1125-1127.
- [5] Waerner T, Alacakaptan M, Tamir I, Oberauer R, Gal A, Brabletz T, Schreiber M, Jechlinger M, Beug H (2006) ILEI: A cytokine essential for EMT, tumor formation, and late events in metastasis in epithelial cells. *Cancer Cell* **10**, 227-239.
- [6] Maatta JA, Bendre A, Laanti M, Buki KG, Rantakari P, Tervola P, Saarimäki J, Poutanen M, Harkonen P, Vaananen K (2016) Fam3c modulates osteogenic cell differentiation and affects bone volume and cortical bone mineral density. *Bonekey Rep* **5**, 787.
- [7] Bendre A, Buki KG, Maatta JA (2017) Fam3c modulates osteogenic differentiation by down-regulating Runx2. *Differentiation* **93**, 50-57.
- [8] Chen Z, Ding L, Yang W, Wang J, Chen L, Chang Y, Geng B, Cui Q, Guan Y, Yang J (2017) Hepatic activation of the FAM3C-HSF1-CaM pathway attenuates hyperglycemia of obese diabetic mice. *Diabetes* **66**, 1185-1197.
- [9] Chen Z, Wang J, Yang W, Chen J, Meng Y, Feng B, Chi Y, Geng B, Zhou Y, Cui Q, Yang J (2017) FAM3C activates HSF1 to suppress hepatic gluconeogenesis and attenuate hyperglycemia of type 1 diabetic mice. *Oncotarget* **8**, 106038-106049.
- [10] Hasegawa H, Liu L, Tooyama I, Murayama S, Nishimura M (2014) The FAM3 superfamily member ILEI ameliorates Alzheimer's disease-like pathology by destabilizing the penultimate amyloid- β precursor. *Nat Commun* **5**, 3917.
- [11] Kamenetz F, Tomita T, Hsieh H, Seabrook G, Borchelt D, Iwatsubo T, Sisodia S, Malinow R (2003) APP processing and synaptic function. *Neuron* **37**, 925-937.
- [12] Cirrito JR, Yamada KA, Finn MB, Sloviter RS, Bales KR, May PC, Schoepp DD, Paul SM, Mennerick S, Holtzman DM (2005) Synaptic activity regulates interstitial fluid amyloid- β levels *in vivo*. *Neuron* **48**, 913-922.
- [13] Sperling RA, Laviolette PS, O'Keefe K, O'Brien J, Rentz DM, Pihlajamäki M, Marshall G, Hyman BT, Selkoe DJ, Hedden T, Buckner RL, Becker JA, Johnson KA (2009) Amyloid deposition is associated with impaired default network function in older persons without dementia. *Neuron* **63**, 178-188.
- [14] Pascoal TA, Mathotaarachchi S, Kang MS, Mohaddes S, Shin M, Park AY, Parent MJ, Benedet AL, Chamoun M, Theriault J, Hwang H, Cuello AC, Misic B, Soucy JP, Aston JAD, Gauthier S, Rosa-Neto P (2019) A β -induced vulnerability propagates via the brain's default mode network. *Nat Commun* **10**, 2353.
- [15] Liu L, Watanabe N, Akatsu H, Nishimura M (2016) Neuronal expression of ILEI/FAM3C and its reduction in Alzheimer's disease. *Neuroscience* **330**, 236-246.
- [16] Saito T, Matsuba Y, Mihira N, Takano J, Nilsson P, Itoharu S, Iwata N, Saido TC (2014) Single App knock-in mouse models of Alzheimer's disease. *Nat Neurosci* **17**, 661-663.
- [17] Takeda S, Sato N, Ikimura K, Nishino H, Rakugi H, Morishita R (2011) Novel microdialysis method to assess neuropeptides and large molecules in free-moving mouse. *Neuroscience* **186**, 110-119.
- [18] Jansson AM, Csiszar A, Maier J, Nystrom AC, Ax E, Johansson P, Schiavone LH (2017) The interleukin-like epithelial-mesenchymal transition inducer ILEI exhibits a non-interleukin-like fold and is active as a domain-swapped dimer. *J Biol Chem* **292**, 15501-15511.
- [19] Kang JE, Lim MM, Bateman RJ, Lee JJ, Smyth LP, Cirrito JR, Fujiki N, Nishino S, Holtzman DM (2009) Amyloid- β dynamics are regulated by orexin and the sleep-wake cycle. *Science* **326**, 1005-1007.
- [20] Cirrito JR, May PC, O'Dell MA, Taylor JW, Parsadanian M, Cramer JW, Audia JE, Nissen JS, Bales KR, Paul SM, DeMattos RB, Holtzman DM (2003) *In vivo* assessment of brain interstitial fluid with microdialysis reveals plaque-associated changes in amyloid- β metabolism and half-life. *J Neurosci* **23**, 8844-8853.
- [21] Hettinger JC, Lee H, Bu G, Holtzman DM, Cirrito JR (2018) AMPA-ergic regulation of amyloid- β levels in an Alzheimer's disease mouse model. *Mol Neurodegener* **13**, 22.
- [22] Whitton PS, Maione S, Biggs CS, Fowler LJ (1994) Tonic desensitization of hippocampal alpha-amino-3-hydroxy-5-methyl-4-isoxazolepropionic acid receptors regulates

- 5-hydroxytryptamine release *in vivo*. *Neuroscience* **63**, 945-948.
- [23] Verges DK, Restivo JL, Goebel WD, Holtzman DM, Cirrito JR (2011) Opposing synaptic regulation of amyloid- β metabolism by NMDA receptors *in vivo*. *J Neurosci* **31**, 11328-11337.
- [24] Beach TG, Kuo YM, Schwab C, Walker DG, Roher AE (2001) Reduction of cortical amyloid β levels in guinea pig brain after systemic administration of physostigmine. *Neurosci Lett* **310**, 21-24.
- [25] Caccamo A, Oddo S, Billings LM, Green KN, Martinez-Coria H, Fisher A, LaFerla FM (2006) M1 receptors play a central role in modulating AD-like pathology in transgenic mice. *Neuron* **49**, 671-682.
- [26] Somogyi P, Tamas G, Lujan R, Buhl EH (1998) Salient features of synaptic organisation in the cerebral cortex. *Brain Res Brain Res Rev* **26**, 113-135.
- [27] Picciotto MR, Higley MJ, Mineur YS (2012) Acetylcholine as a neuromodulator: Cholinergic signaling shapes nervous system function and behavior. *Neuron* **76**, 116-129.
- [28] Saura CA, Chen G, Malkani S, Choi SY, Takahashi RH, Zhang D, Gouras GK, Kirkwood A, Morris RG, Shen J (2005) Conditional inactivation of presenilin 1 prevents amyloid accumulation and temporarily rescues contextual and spatial working memory impairments in amyloid precursor protein transgenic mice. *J Neurosci* **25**, 6755-6764.
- [29] Willen K, Sroka A, Takahashi RH, Gouras GK (2017) Heterogeneous association of Alzheimer's disease-linked amyloid- β and amyloid- β protein precursor with synapses. *J Alzheimers Dis* **60**, 511-524.
- [30] Half AW, Gomez-Varela D, John D, Berg DK (2014) A novel mechanism for nicotinic potentiation of glutamatergic synapses. *J Neurosci* **34**, 2051-2064.
- [31] Koukouli F, Rooy M, Changeux JP, Maskos U (2016) Nicotinic receptors in mouse prefrontal cortex modulate ultraslow fluctuations related to conscious processing. *Proc Natl Acad Sci U S A* **113**, 14823-14828.
- [32] Rice HC, Marcassa G, Chrysidou I, Horre K, Young-Pearse TL, Muller UC, Saito T, Saido TC, Vassar R, de Wit J, De Strooper B (2020) Contribution of GABAergic interneurons to amyloid- β plaque pathology in an APP knock-in mouse model. *Mol Neurodegener* **15**, 3.
- [33] Rodrigues DI, Gutierrez J, Pliassova A, Oliveira CR, Cunha RA, Agostinho P (2014) Synaptic and sub-synaptic localization of amyloid- β protein precursor in the rat hippocampus. *J Alzheimers Dis* **40**, 981-992.
- [34] Nordberg A, Hellstrom-Lindahl E, Lee M, Johnson M, Mousavi M, Hall R, Perry E, Bednar I, Court J (2002) Chronic nicotine treatment reduces β -amyloidosis in the brain of a mouse model of Alzheimer's disease (APPsw). *J Neurochem* **81**, 655-658.
- [35] Echeverria V, Zeitlin R, Burgess S, Patel S, Barman A, Thakur G, Mamcarz M, Wang L, Sattelle DB, Kirschner DA, Mori T, Leblanc RM, Prabhakar R, Arendash GW (2011) Cotinine reduces amyloid- β aggregation and improves memory in Alzheimer's disease mice. *J Alzheimers Dis* **24**, 817-835.
- [36] Lassek M, Weingarten J, Einsfelder U, Brendel P, Muller U, Volkandt W (2013) Amyloid precursor proteins are constituents of the presynaptic active zone. *J Neurochem* **127**, 48-56.
- [37] Ludewig S, Korte M (2016) Novel insights into the physiological function of the APP (gene) family and its proteolytic fragments in synaptic plasticity. *Front Mol Neurosci* **9**, 161.
- [38] Barthet G, Jorda-Siquier T, Rumi-Masante J, Bernadou F, Muller U, Mülle C (2018) Presenilin-mediated cleavage of APP regulates synaptotagmin-7 and presynaptic plasticity. *Nat Commun* **9**, 4780.